

Hybrid skin-topological modes without asymmetric couplings

Weiwei Zhu^{1,*} and Jiangbin Gong^{1,†}

¹*Department of Physics, National University of Singapore, 117542, Singapore*

Abstract: Non-Hermitian skin effect (NHSE) in non-Hermitian lattice systems, associated with a point gap on the complex energy plane, has attracted great theoretical and experimental interest. Much less is studied on the so-called second-order non-Hermitian skin effect, where the bulk does not support a point gap but localization at the corner still occurs. This work discovers a class of hybrid skin-topological modes as the second-order non-Hermitian skin effect without asymmetric couplings. Specifically, by only adding gain/loss to two-dimensional Chern insulators and so long as the gain/loss strength does not close the line gap, all the topological edge states are localized at one corner under the open boundary condition, with the bulk states extended. The resultant non-Hermitian Chern bands can be still topologically characterized by Chern numbers, whereas the hybrid skin-topological modes are understood via some auxiliary Hermitian systems that belong to either intrinsic or extrinsic second-order topological insulator phases. By proposing an innovative construction of auxiliary Hamiltonian, our generic route to hybrid skin-topological modes is further successfully extended to nonequilibrium topological systems with gain and loss, where the anomalous Floquet band topology is no longer captured by band Chern numbers. The extension thus leads to the intriguing finding of nonequilibrium hybrid skin-topological modes. In addition to offering a straightforward route to experimental realization of hybrid topological-skin effects, this study also opens up a promising perspective for the understanding of corner localization by revealing the synergy of three important concepts, namely, non-Hermitian topological insulator, second-order non-Hermitian skin effect, and second-order topological insulator.

Keywords: second-order non-Hermitian skin effect, non-Hermitian Chern insulator, second-order topological insulator, nonequilibrium hybrid skin-topological modes.

INTRODUCTION

Non-Hermitian systems are now widely known to support topological states that may not exist in Hermitian system [1–3]. The bulk spectrum of non-Hermitian lattice systems under the periodic boundary condition (PBC) is typically complex, and the gap can be either a line gap or a point gap. Different gaps associated with specific symmetries can then be used to classify a wide variety of non-Hermitian topological phases [4, 5]. Though line-gap topology may be transformed to a Hermitian counterpart without closing the band gap, point-gap topology is unique to non-Hermitian systems. In particular, point-gap topology is the underlying topological protection responsible for the so-called non-Hermitian skin effect (NHSE) [6, 7], causing all the bulk states to be localized under the open boundary condition (OBC) [8–20].

NHSE, as guaranteed by a point-gap topology, has spurred a great deal of theoretical interest because it breaks the usual bulk-edge correspondence for line-gap topology [21, 22]. Indeed, non-Bloch topological band theory has been developed to recover the bulk-edge correspondence for non-Hermitian systems [8, 23–37]. A variety of physical platforms, such as cold atoms, photonics, electrical circuits, mechanics, and acoustics have been de-

veloped to study NHSE experimentally, with motivating findings [38–48].

It is fair to say that most studies to date have focused on NHSE in one-dimensional (1D) systems. In other case studies that do involve two-dimensional (2D) systems, the interplay of NHSE and topological bands is already found to bring interesting physics, such as non-Hermitian Chern bands [23, 49–53], defect induced NHSE [54–57], and the hybrid skin-topological modes [17, 46, 58, 59] where corner localization is due to the interplay of topological localization and NHSE. Nevertheless, as far as NHSE is concerned in these studies of 2D systems, it is essentially the 1D (or first-order) NHSE that is in force, because the source of NHSE can be clearly attributed to one direction, but not the other direction. In particular, to date our knowledge of hybrid skin-topological mode is based on a specific lattice design [17, 58], namely, the manifestation of asymmetric coupling in one direction in the presence of topological localization in the other direction.

There have also been growing interest in the so-called second-order NHSE that can localize certain states at the corner while all the bulk states are still extended under OBC [60–63]. Second-order NHSE is remarkable because the bulk band does not even support a point gap, so the resulting skin corner modes are clearly beyond the usual paradigm of NHSE. A point gap now emerges only after one of the dimensions is placed under OBC and the second dimension is under PBC. This being the case, skin corner modes can be obtained after placing two differ-

* phyzhuw@gmail.com

† phygj@nus.edu.sg

ent dimensions under OBC, hence of second-order. Such type of skin corner modes is of second-order for another physical reason. That is, available studies [60–63] indicate that second-order NHSE can be connected with a second-order topological insulator phase of some auxiliary Hamiltonian. However, all theoretical models proposed to date require asymmetric couplings (plus, positive couplings along one direction and negative couplings along another direction). These constructions are convenient in theory, but far from trivial in experimental realizations.

Echoing with the possibility of inducing non-Hermitian topological phase transitions solely by gain and loss [64–69], in this work we shall reveal a generic route to hybrid skin-topological modes without asymmetric couplings, by applying solely gain and loss to topological insulators with chiral edge states, for both conventional Chern insulator phases and periodically driven (hence nonequilibrium) topological phases. The subtle interplay between topology and non-Hermitian effects then leads to hybrid skin-topological modes, which can be identified as a new type of second-order NHSE. In particular, upon the introduction of some gain and loss that still maintains the line-gap topology of the starting topological insulator phase, the system continues to support chiral edge states, which now however acquire gain and loss as they propagate along the edges of the system. For example, in the case of a non-Hermitian Chern insulator, it is still topologically described by a non-zero Chern number upon introducing gain and loss. Remarkably, we show that skin corner modes generically exist under OBC, with their number being proportional to the length of a 2D system and localized at one corner of the system only. As shown below, the localization behavior of the obtained corner skin models can be phenomenologically understood by state accumulation of chiral edge states with gain and loss. Furthermore, the existence of corner skin models can also be understood through the construction of an auxiliary Hamiltonian [70–84]. That is, the non-Hermitian systems under consideration must host skin corner modes if the auxiliary Hamiltonian is in a second-order topological insulator phase, protected by a bulk gap (intrinsic second-order) or an edge-state gap inside the bulk gap (extrinsic second-order) [85]. In either case the introduced gain and loss can induce an edge band gap opening and thus a phase transition to the second-order topological insulating phase. We also show that the nature of hybrid skin-topological modes allows for the construction of a topological switch to turn on/off skin effects, simply by introducing topological phase transitions.

As compared with the asymmetric couplings previously assumed in second-order NHSE or hybrid skin-topological modes [17, 46, 58, 59], the physics revealed in this work is widely applicable because gain or loss is much easier to realize. As a matter of fact, loss is ubiquitous due to absorbing materials or some leaky modes,

and gain can also be introduced by optical or electrical pumping in photonic systems. Because our route to hybrid skin-topological modes is rather general, we are motivated to explore the possibility of nonequilibrium skin-topological modes. We indeed manage to extend our approach to nonequilibrium topological systems with gain and loss, where the anomalous Floquet band topology is no longer captured by band Chern numbers. To better connect nonequilibrium hybrid skin-topological modes with second-order topology, we have proposed an innovative construction of auxiliary Hamiltonian to treat periodically driven topological systems with gain and loss.

HYBRID SKIN-TOPOLOGICAL MODES IN A NON-HERMITIAN HALDANE MODEL

Haldane model with gain and loss

We start with a non-Hermitian Haldane model, as depicted in Fig. 1(a). This non-Hermitian version of the Haldane model is obtained by introducing gain and loss to two sublattices respectively [86]. The resulting tight-binding lattice Hamiltonian can be expressed as follows:

$$H = t_1 \sum_{\langle i,j \rangle} c_i^\dagger c_j + t_2 e^{i\nu_{ij}\phi} \sum_{\langle\langle i,j \rangle\rangle} c_i^\dagger c_j + ig \sum_{i \in A} c_i^\dagger c_i - ig \sum_{i \in B} c_i^\dagger c_i \quad (1)$$

where c_i^\dagger (c_i) is the creation (annihilation) operator for a particle at the i th site. The first term is the nearest-neighbor hopping with an amplitude t_1 . The second term is the next-nearest-neighbor hopping with an amplitude t_2 and a phase $\nu_{ij}\phi$. The phase is direction dependent. If the hopping is along the arrows in Fig. 1(a), the phase is positive $\nu_{ij} = +1$. If the hopping is in the opposite direction, the phase is negative $\nu_{ij} = -1$. The second term breaks the time reversal symmetry so that the system can support quantum anomalous Hall effect. The third term is what we introduce in this work, representing the on-site gain (loss) on sublattice A (sublattice B). In the absence of such gain and loss, the system is a well-known Chern insulator and supports topological chiral edge states.

As a rather standard treatment, one can now apply a Fourier transformation to the real-space Hamiltonian in Eq. 1, obtaining the momentum-space Hamiltonian:

$$H(\mathbf{k}) = \vec{d}(\mathbf{k}) \cdot \vec{\sigma} + ig\sigma_z \quad (2)$$

where $\vec{d}(\mathbf{k}) = (d_0(\mathbf{k}), d_x(\mathbf{k}), d_y(\mathbf{k}), d_z(\mathbf{k}))$ is a vector as

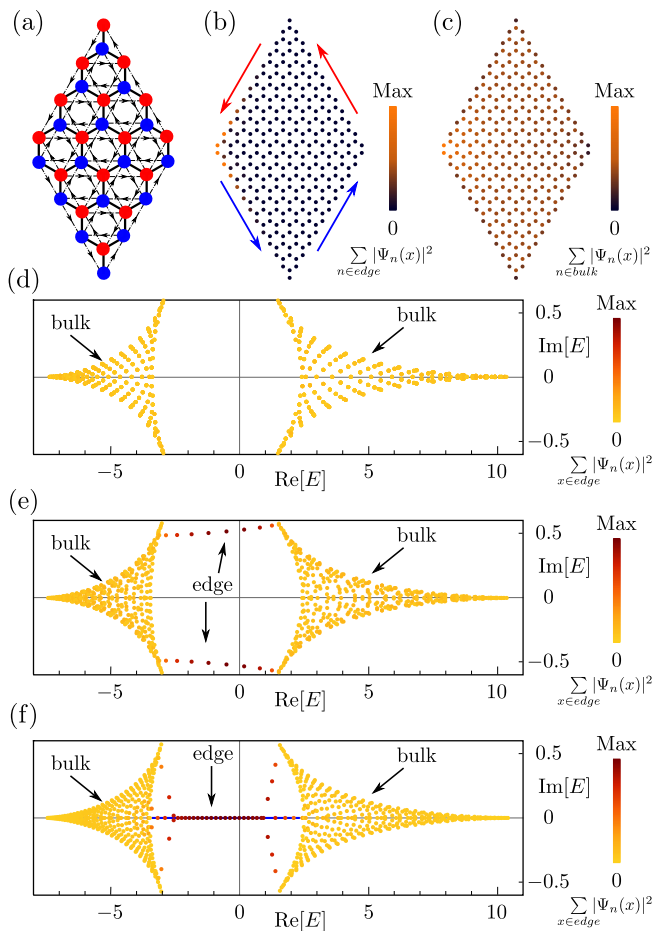


FIG. 1. (Color online) Hybrid skin-topological modes as a second-order non-Hermitian skin effect in a non-Hermitian Haldane model. (a) Non-Hermitian Haldane model with gain (blue) and loss (red). (b) Summation of the state density profile over all edge states $\sum_{n \in \text{edge}} |\Psi_n(x)|^2$. Color represents the strength of localization on the left edge $\sum_{x \in \text{edge}} |\Psi_n(x)|^2$. (c) Summation of the state density profile over all bulk states $\sum_{n \in \text{bulk}} |\Psi_n(x)|^2$. Color represents the strength of localization of all the bulk states $\sum_{x \in \text{bulk}} |\Psi_n(x)|^2$. (d) Spectrum of the system under PBC along both directions. Color represents the strength of localization on the left edge $\sum_{x \in \text{edge}} |\Psi_n(x)|^2$. (e) Spectrum of a semi-infinite structure with PBC along x and OBC along y . Color represents the strength of localization on the left edge $\sum_{x \in \text{edge}} |\Psi_n(x)|^2$. (f) Spectrum of a finite structure with OBC along both directions. Color represents the strength of localization on the left edge $\sum_{x \in \text{edge}} |\Psi_n(x)|^2$.

function of \mathbf{k} , $\vec{\sigma} = (\sigma_0, \sigma_x, \sigma_y, \sigma_z)$ and

$$\begin{aligned}
 d_0(\mathbf{k}) &= 2t_2 \cos \phi [\cos k_x + 2 \cos(k_x/2) \cos(\sqrt{3}k_y/2)], \\
 d_x(\mathbf{k}) &= t_1 [1 + 2 \cos(k_x/2) \cos(\sqrt{3}k_y/2)], \\
 d_y(\mathbf{k}) &= 2t_1 \cos(k_x/2) \sin(\sqrt{3}k_y/2), \\
 d_z(\mathbf{k}) &= -2t_2 \sin \phi [\sin k_x + 2 \sin(k_x/2) \cos(\sqrt{3}k_y/2)],
 \end{aligned} \tag{3}$$

with $\mathbf{k} = (k_x, k_y)$ being quasimomentum, σ_0 being two-by-two identity matrix and σ_i , $i = x, y, z$ being the Pauli matrices.

Let us first investigate the spectrum of the above-described non-Hermitian Haldane model under the open boundary condition (OBC). In our sample calculations, we use the following system parameters $t_1 = 3$, $t_2 = 0.5$, $g = 0.6$ and $\phi = \pi/3$ unless specified otherwise. For zero gain and loss, the model system here is a Chern insulator with chiral edge states propagating along the system's edge with a definite direction due to time-reversal-symmetry breaking [86]. Upon introduction of the gain and loss to two sublattices, it is expected that there will be no band gap closure so long as the strength of the gain and loss terms is not too strong. Remarkably, all the identified topological edge states in the bulk gap are found to be localized at the system's left corner, as shown in Fig. 1(b) whereas all the bulk states are extended as shown in Fig. 1(c). Furthermore, without a line-gap topological transition, the system in the presence of the gain and loss is still classified as a Chern insulator, but as a non-Hermitian version. Fig. 1(d)-(f) compare the spectrum plotted on the complex energy plane under PBC, mixed PBC-OBC, and OBC. The PBC spectrum in Fig. 1(d) depicts two well-separated bulk bands. The spectrum of the system of a semi-infinite (strip) structure in Fig. 1(e) shows that the chiral edge states together with the bulk spectrum encloses a nonzero area, thus potentially allowing a point gap. In Fig. 1(f) for the system under OBC, two well-separated bulk bands are seen. Between the two bulk bands in Fig. 1(f), there are gapless topological edge states connecting the two bulk gaps. That the energies of the chiral edge states here are dramatically different when we change the boundary condition from mixed PBC-OBC to OBC strongly suggests that the observed corner modes here are due to the skin localization of chiral edge states and hence represent hybrid skin-topological modes.

It is now necessary to digest why the topological chiral edge states are all localized at one corner of the system. To that end we next look into more details of the energy bands of this system in a zigzag strip structure with periodic boundary condition (PBC) along x and OBC along y . The real part and imaginary parts of the complex spectrum under such a mixed PBC-OBC boundary condition are shown in Fig. 2(a) and Fig. 2(b), respectively, as a function of the Bloch momentum k_x along the x direction. From Fig. 2(a) and Fig. 2(b) one clearly sees that there are two topological edge channels marked by red color and blue color. The red one represents the edge channel propagating towards the left direction with gain (because of the positive imaginary part), whereas the blue one represents the edge channel that only allows transport to the right with loss (because of the negative imaginary part). To reflect this observation, in Fig. 1(b) we further mark the gain edge states and loss edge states

by blue arrows and red arrows. Evidently, then, as gain edge states propagate to the left with gain, it tends to accumulate population on the left corner. Interestingly and analogously, because the loss edge state propagate to the right with loss, the loss edge states prefer to accumulate to the left corner. Thus, no matter what edge state channels we inspect, they all tend to be localized at the left corner. This is a noteworthy feature of the system and can only be taken as a phenomenological explanation of why skin corner modes should generically emerge in a non-Hermitian Chern insulator.

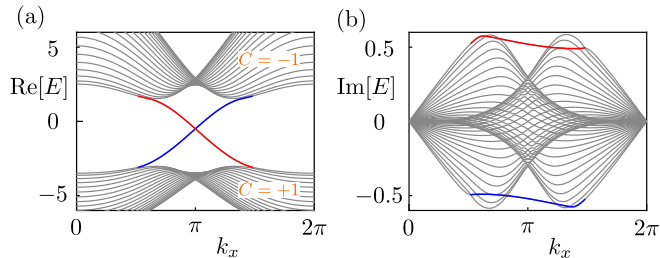


FIG. 2. (Color online) Topological edge states of a non-Hermitian Haldane model in a zigzag strip structure. (a) Real part of the energy bands. (b) Imaginary part of the energy bands. Note that the edge states propagate to the left has positive imaginary parts and hence acquire gain, and the edge states propagate to the right has negative imaginary parts and hence experience loss.

The non-Hermitian Haldane model thus depicts a non-Hermitian Chern insulator, of which the topological characterization can be captured by the following Chern number defined as [23]

$$C_n = \frac{1}{2\pi i} \int_{BZ} d^2\mathbf{k} \epsilon_{ij} \langle \partial_i u_{Ln}(\mathbf{k}) | \partial_j u_{Rn}(\mathbf{k}) \rangle \quad (4)$$

where n is the band number, $i, j = x, y$ and $\epsilon_{xy} = -\epsilon_{yx} = 1$. $|u_{Ln}(\mathbf{k})\rangle$ and $|u_{Rn}(\mathbf{k})\rangle$ are left and right eigenvectors of $H(\mathbf{k})$ with normalization condition $\langle u_{Ln}(\mathbf{k}) | u_{Rn}(\mathbf{k}) \rangle = 1$. Because all the bulk bands here are extended, the conventional (first-order) NHSE is not manifested by the bulk bands under PBC and hence the non-Hermitian band Chern numbers can be defined in the usual Brillouin zone, without invoking the so-called non-Bloch Chern number in the generalized Brillouin zone. Indeed, the Chern numbers for the two bands based on the usual Brillouin zone are ± 1 , as shown in Fig. 2(a). The conventional bulk-boundary correspondence is also obeyed: there are two chiral edge channels in the band gap, as shown in Fig. 2, propagating towards opposite directions and found at opposite edges of the strip geometry.

Topological characterization of hybrid skin-topological modes

The topological Chern numbers discussed at the end of the previous section can be used to understand the bulk-edge correspondence of the non-Hermitian Chern insular in a strip geometry. However, it remains to establish the bulk-corner correspondence in order to reveal the nature of hybrid skin-topological modes discovered above. For conventional (first-order) NHSE, it is known to have a topological origin and can be associated with some nonzero winding number of the spectrum on the complex plane [6, 7]. By analogy, the skin corner modes arising from the localization of chiral edge modes can be associated with some nonzero spectral winding number of non-Hermitian chiral edge states. However, in practice it is not an easy task to solely extract the edge states to facilitate the calculation of the spectral winding number of the edge states. This is most obvious if we return to the spectrum shown in Fig. 1(e), where the energies of the edge states at the opposite sides of a strip structure are connected with delocalized states and hence there is no distinct closed spectral loops. Physically, this is because the edge states at one side of the strip cannot be adiabatically connected with (or pumped to) those at the other side, unless there is a delocalization transition through the bulk states.

Following Refs. [60–62], below we turn to an auxiliary Hamiltonian approach in order to reveal the nature of the found hybrid skin-topological modes induced by gain and loss in the Haldane model $H(\mathbf{k})$. Specifically, let us consider the following Hamiltonian constructed from $H(\mathbf{k})$,

$$\tilde{H}(\mathbf{k}, E_r) = \begin{pmatrix} 0 & H(\mathbf{k}) - E_r \\ H^\dagger(\mathbf{k}) - E_r & 0 \end{pmatrix}, \quad (5)$$

with E_r being a real number and representing a reference energy. As seen above, the auxiliary Hamiltonian is Hermitian by construction. Specifically, $\tilde{H}(\mathbf{k}, E_r)$ lives on the expanded Hilbert space, the tensor product of the Hilbert space of $H(\mathbf{k})$ and that of an additional fictitious pseudo-spin degree of freedom, depicted by another set of three Pauli matrices τ_j , $j = x, y, z$. The above-defined auxiliary Hamiltonian can then be written as

$$\tilde{H}(\mathbf{k}, E_r) = \tau_+(H(\mathbf{k}) - E_r) + \tau_-(H^\dagger(\mathbf{k}) - E_r) \quad (6)$$

$\tau_\pm = \tau_x \pm \tau_y$. It is then seen clearly that the auxiliary Hermitian Hamiltonian satisfies the following chiral symmetry

$$\tau_z \tilde{H}(\mathbf{k}, E_r) \tau_z = -\tilde{H}(\mathbf{k}, E_r). \quad (7)$$

The usefulness of the above-constructed auxiliary Hamiltonian can be appreciated as follows. Consider 1D Hermitian systems with chiral symmetry, where the

pseudo-spin degree of freedom is defined via τ_j , $j = x, y, z$. The emergence of topological zero modes in such 1D systems is protected by a non-zero winding of vector $\{\Re[Q(k)] - E_r, \Im[Q(k)]\}$ around the origin of complex plane. Here $Q(k) = \det[H(\mathbf{k})]$ being the determinant of $H(\mathbf{k})$ is a complex number. For example, for the 1D Su-Schrieffer-Heeger (SSH) model $H_{\text{SSH}} = h_x(k)\tau_x + h_y(k)\tau_y$, the existence of topological zero modes can be directly connected, via the well-known bulk-edge correspondence, with the winding of the 2D vector $[h_x(k), h_y(k)]$ around the origin as the 1D momentum k is scanned across the whole Brillouin zone. With this preparation, let us now return to our 2D auxiliary model system but with mixed boundary condition, namely, one direction is open and the second direction is under PBC, with k_{\parallel} being the Bloch momentum parallel to the edge. Let us further assume that the edge Hamiltonian of this 2D system is now reduced to

$$\tilde{H}_{\text{edge}}(k_{\parallel}, E_r) = \tau_+(H_{\text{edge}}(k_{\parallel}) - E_r) + \tau_-(H_{\text{edge}}^{\dagger}(k_{\parallel}) - E_r), \quad (8)$$

which can be understood in parallel with a 1D model with chiral symmetry. Let $Q_{\text{edge}}(k) = \det[H_{\text{edge}}(k_{\parallel})]$. One can then infer that the nontrivial winding of $\{\Re[Q_{\text{edge}}(k_{\parallel})], \Im[Q_{\text{edge}}(k_{\parallel})]\}$ around E_r has a definite correspondence with the emergence of topological edge modes of the edge Hamiltonian (hence topological corner modes, if the k_{\parallel} direction is also opened up). Thus, the emergence of topological corner modes for the system $\tilde{H}(\mathbf{k}, E_r)$ under OBC reflects the winding of $\{\Re[Q_{\text{edge}}(k_{\parallel})], \Im[Q_{\text{edge}}(k_{\parallel})]\}$ around E_r . Remarkably, precisely it is the winding behavior of $\{\Re[Q_{\text{edge}}(k_{\parallel})], \Im[Q_{\text{edge}}(k_{\parallel})]\}$ around E_r that one needs in order to confirm the occurrence of skin effects on the chiral edge states of the original non-Hermitian Chern insulator when the second direction is also placed under OBC.

Insights above have made it clear the following bulk-edge-corner correspondence: If $H_{\text{edge}}(k_{\parallel})$ indeed has non-zero spectral winding number for the chiral edge states, or equivalently, if the auxiliary Hermitian Hamiltonian $\tilde{H}(\mathbf{k}, E_r)$ is actually a second-order topological insulator supporting topological corner modes, then under OBC in both directions, the non-Hermitian Chern insulator $H(\mathbf{k})$ hosts corner skin modes. We are now ready to carry out a detailed analysis of the auxiliary Hamiltonian $\tilde{H}(\mathbf{k}, E_r)$. By substituting Eq. (2) into Eq. (5), the explicit auxiliary Hamiltonian for our non-Hermitian Haldane model reads as follows:

$$\tilde{H}(\mathbf{k}, E_r) = [d_0(\mathbf{k}) - E_r]\tau_x\sigma_0 + d_x(\mathbf{k})\tau_x\sigma_x + d_y(\mathbf{k})\tau_x\sigma_y + d_z(\mathbf{k})\tau_x\sigma_z + g\tau_y\sigma_z. \quad (9)$$

Here the second and third terms yield Dirac points at some high-symmetry momentum points. Interestingly, the fourth term opens a band gap and gives rise to gapless edge states. The first term commutes with these

three terms so that it just shifts the gapless edge state. In the absence of any gain or loss, the auxiliary Hamiltonian hence supports gapless edge states. The gray lines shown in Fig. 3(a) show one such example with $E_r = -t_2$. In particular, the existence of gapless edge states clearly indicates that the auxiliary Hamiltonian without gain or loss is a first-order topological insulator. Intriguing physics sets in when gain and loss are introduced. It is seen from Fig. 3(a) (blue lines) that the edge states will acquire a band gap, hinting that the gain and loss introduced here, no matter how weak their strength is, can in fact induce a topological phase transition. Indeed, the gain/loss term is reflected in the fifth term in Eq. 9, which anti-commutes with the fourth term. The gain/loss scheme advocated here is hence the main reason to induce gapped edge states, one main feature of second-order topological insulators.

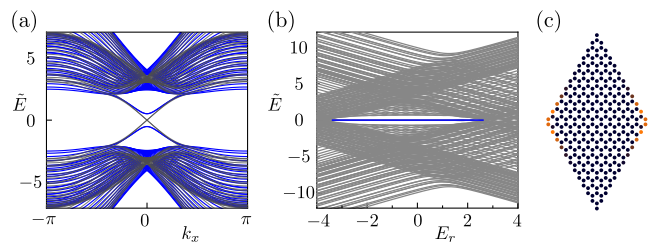


FIG. 3. (Color online) Second-order topological insulator of the auxiliary Hamiltonian defined in the main text. (a) Energy bands of zigzag strip structure. Gray (blue) lines show the results without (with) gain and loss, $g = 0$ ($g = 0.6$). (b) Spectrum of finite structure as a function of reference energy E_r . (c) State density profile for the topological zero-energy corner states with $E_r = -t_2$.

To strengthen our findings on corner skin modes that can be obtained only under OBC for both dimensions, next we further confirm that the auxiliary Hermitian Hamiltonian $\tilde{H}(\mathbf{k}, E_r)$ is a second-order topological insulator by symmetry analysis and spectrum calculations. Firstly, note that $H(\mathbf{k})$ supports pseudo inversion symmetry $\sigma_x H(\mathbf{k}) \sigma_x = H^{\dagger}(-\mathbf{k})$ so that the auxiliary Hamiltonian are inversion-symmetric, namely, $I \tilde{H}(\mathbf{k}, E_r) I^{-1} = \tilde{H}(-\mathbf{k}, E_r)$ with $I = \tau_x \sigma_x$. Upon a symmetry analysis applied to two lower bands at inversion symmetric momentum points, it is found that the auxiliary Hermitian Hamiltonian here does not have the Wannier representation. However, it can be Wannierized by adding a trivial atomic insulator $s@q_{1c}$ [87] and is hence a fragile topological phase, which can be expressed as $s@q_{1b} \oplus p@1_{1a} \oplus p@q_{1d} \ominus s@q_{1c}$ (See Appendix A). Such fragile topological phase has half topological charge at the left and right corners. Combined with the above-identified chiral symmetry, this auxiliary system can be predicted to support topological zero-energy corner modes [88]. Fig. 3(b) presents the spectrum of the auxiliary system with OBC in both directions, as a function

of E_r . The auxiliary system is seen to support topological zero-energy states in the range of $-3.5 \lesssim E_r \lesssim 2.5$, which agrees perfectly with the spectrum of the skin corner modes of our non-Hermitian Chern insulator under OBC, as shown in Fig. 1(f). Fig. 3(c) further presents state density profiles of the found topological zero-energy states of $\tilde{H}(\mathbf{k}, E_r)$, with $E_r = -t_2$. These topological states are indeed localized at the corners and hence are second-order topological corner states. This comparison in terms of the zero-energy states between the auxiliary system and our actual non-Hermitian Chern insulator verifies our physical insights above.

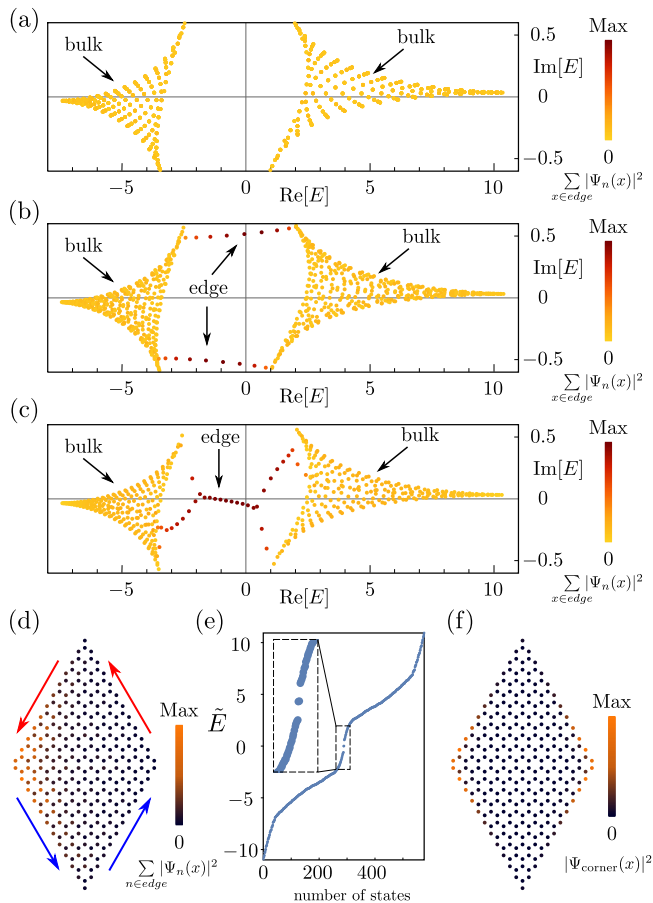


FIG. 4. Spectrum and hybrid skin-topological modes in a non-Hermitian Haldane model with on-site potential difference introduced. (a)-(c): Spectrum of the system under PBC, mixed PBC-OBC, and OBC, respectively. Color represents the strength of localization on the left edge $\sum_{x \in \text{edge}} |\Psi_n(x)|^2$. (d) Summation of state densities for all edge states $\sum_{n \in \text{edge}} |\Psi_n(x)|^2$. (e) Spectrum of the constructed auxiliary Hamiltonian. (f) The profile of zero-energy topological corner mode shown in (e) In all the calculations, μ is chosen as 0.5.

Our discussions so far have connected with the hybrid skin-topological modes with an auxiliary Hamiltonian as a second-order topological insulator protected by

inversion symmetry and chiral symmetry. The involved second-order topological insulator phase is of the intrinsic type, because this phase is protected by the bulk topology with crystal symmetry, and so no topological phase transitions can occur without bulk-gap closing or symmetry breaking. This brings us an interesting question as follows: is it possible to have hybrid skin-topological modes with a second-order topological insulator of the extrinsic type, where the second-order topological phase is only protected by a gap of the edge states or by the edge topology [85].

To address this interesting question we now introduce a weak on-site potential difference ($\mu \sum_{i \in A} c_i^\dagger c_i - \mu \sum_{i \in B} c_i^\dagger c_i$) to Eq. (1). This additional term breaks the pseudo inversion symmetry of $H(\mathbf{k})$ so that it also breaks the inversion symmetry of the associated auxiliary Hamiltonian. Without such crystal symmetry, the obtained second-order topological insulator phase is not protected by a bulk gap.

Consider then first the spectrum of the system $H + \mu \sum_{i \in A} c_i^\dagger c_i - \mu \sum_{i \in B} c_i^\dagger c_i$, under PBC, mixed PBC-OBC, and OBC, as shown in Fig. 4(a)-(c). The main spectral features observed in the previous case are also observed here. Fig. 4(a) depicts two bulk bands under PBC. Under mixed PBC-OBC in Fig. 4(b), edge states are observed on top of the bulk spectrum, with the whole spectrum enclosing a nonzero area. The energetics of the edge states change dramatically again when we change from mixed PBC-OBC to OBC in Fig. 4(c). Interestingly, regardless of the boundary condition, the bulk states are always extended. Fig. 4(d) shows that the edge states are localized at one corner when the system is under OBC.

To verify that these states localized at corner arise from NHSE, we investigate in parallel the spectrum and localization behavior of the corresponding auxiliary Hamiltonian. The spectrum of the auxiliary Hamiltonian under OBC is shown in Fig. 4(e), with in-gap states observed. However, due to the lack of the inversion symmetry possessed in the previous case, the in-gap states are only protected by a gap in the edge states, not by the bulk gap. That is, the presence of edge states is not in one-to-one correspondence with bulk gap closure/opening. The in-gap states can thus only be interpreted as the edge states of 1D edge states and hence the auxiliary Hamiltonian is an extrinsic second-order topological insulator. Nevertheless, Fig. 4(f) verifies that this auxiliary Hamiltonian does support second-order corner modes. The agreement is also checked quantitatively, insofar as the auxiliary Hamiltonian only supports topological zero-energy states in the range of $-3.2 \lesssim E_r \lesssim 2.2$ (See Appendix B), fully consistent with the energetics of the corner states shown in Fig. 4(c).

The hybrid skin-topological corner modes revealed in this work suggests that we may envision the construction of a topological switch to turn on/off the skin effect via

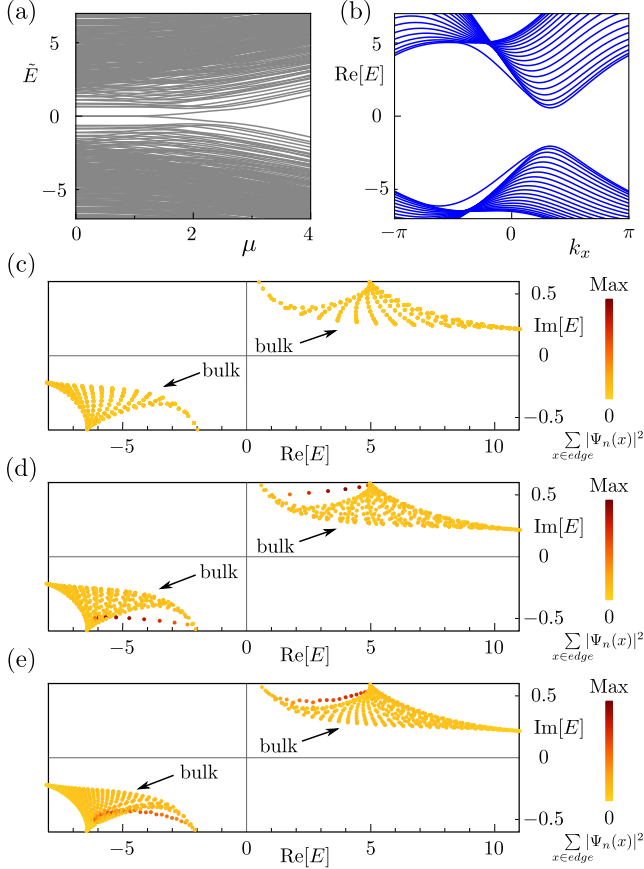


FIG. 5. Topological phase transition causing hybrid skin-topological modes to disappear, thus offering a topological switch to control skin effects. (a) Spectrum of the auxiliary Hamiltonian associated with our non-Hermitian Haldane model, where an on-site potential difference with a varying strength parameter μ is introduced, with fixed $E_r = 0$. (b) Real part of the energy bands for our non-Hermitian Haldane model vs Bloch momentum k_x under mixed PBC-OBC. (c)-(e): Spectrum of the system plotted on the complex energy plane, under PBC, mixed PBC-OBC, and OBC, respectively. Color represents the strength of localization on the left edge $\sum_{x \in \text{edge}} |\Psi_n(x)|^2$. μ is chosen as 3.5 for panels (b)-(e).

topological phase transitions. To explore this possibility, we tune the above-introduced on-site potential difference μ to induce a topological phase transition, from a Chern insulator to a normal insulator. With this topological phase transition, the underlying mechanism for hybrid skin-topological corner modes ceases to exist and hence the skin effect should disappear as well. Fig. 5(a) depicts this topological phase transition via the spectrum of the auxiliary Hamiltonian. Specifically, the auxiliary systems changes from a second-order topological insulator to a normal insulator with the increase of μ , with the topological phase transition point at around $\mu \approx 2$. Taking the case of $\mu = 3.5$ as an example, the non-Hermitian Haldane model introduced here features a normal insulator, as shown in Fig. 5(b) with no gapless topological

chiral edge states. The overall spectrum under PBC, mixed PBC-OBC, and OBC of our system is shown in Fig. 5(c)-(e) on the complex plane. It is now seen that not only the bulk states are insensitive to the boundary conditions, but also the edge states become insensitive to the boundary conditions. Consistent with these observations, hybrid skin-topological modes are not obtained. This strengthens our understanding of the newly discovered class of hybrid skin-topological modes. Indeed, the edge states seen in Fig. 5(d)-(e) are just defect states and not chiral (unidirectional), and hence there will not be net accumulation of gain or loss for these defect states.

NONEQUILIBRIUM HYBRID SKIN-TOPOLOGICAL MODES

Hybrid skin-topological modes in a non-Hermitian periodically driven model

To further confirm that our route towards the hybrid skin-topological modes is widely applicable, we now apply the same strategy to periodically driven (Floquet) topological phases [90–100]. Given that nonequilibrium topological matter is less well understood due to the possibility of anomalous chiral edge states. It is indeed timely to investigate the consequences of adding gain and loss to Floquet topological matter. To our knowledge, so far there is no study whatsoever on hybrid skin-topological modes in nonequilibrium systems.

Without loss of generality, let us consider a model of anomalous Floquet topological phase, as first proposed by in Ref. [89]. This model can be realized with an explicit platform, i.e., coupled ring resonators [81, 101, 102]. The time-dependent Bloch Hamiltonian consists of four steps,

$$H(\mathbf{k}, t) = \begin{cases} H_1(\mathbf{k}) & 0 < t \leq T/4, \\ H_2(\mathbf{k}) & T/4 < t \leq T/2, \\ H_3(\mathbf{k}) & T/2 < t \leq 3T/4, \\ H_4(\mathbf{k}) & 3T/4 < t \leq T, \end{cases} \quad (10)$$

where

$$H_m(\mathbf{k}) = 4 * \theta(e^{ib_m \cdot \mathbf{k}} \sigma^+ + h.c.) + ig\sigma_z, \quad (11)$$

for $m = 1, 2, 3, 4$. Here $\sigma^+ = (\sigma_x + i\sigma_y)/2$ and the vectors \mathbf{b}_m are given by $\mathbf{b}_1 = (0, 0)$, $\mathbf{b}_2 = (1/\sqrt{2}, 1/\sqrt{2})$, $\mathbf{b}_3 = (0, \sqrt{2})$ and $\mathbf{b}_4 = (-1/\sqrt{2}, 1/\sqrt{2})$. We set $T = 1$. As also seen above, the gain and loss are also introduced to two sublattice through the term $ig\sigma_z$. Fig. 6(a) illustrates this nonequilibrium topological phase model.

The quasi-energy Floquet bands $\varepsilon(\mathbf{k})$ of the above-described nonequilibrium system can be obtained by solving the following eigen-equation,

$$U_T(\mathbf{k}) |\Psi(\mathbf{k})\rangle = e^{-i\varepsilon(\mathbf{k})T} |\Psi(\mathbf{k})\rangle, \quad (12)$$

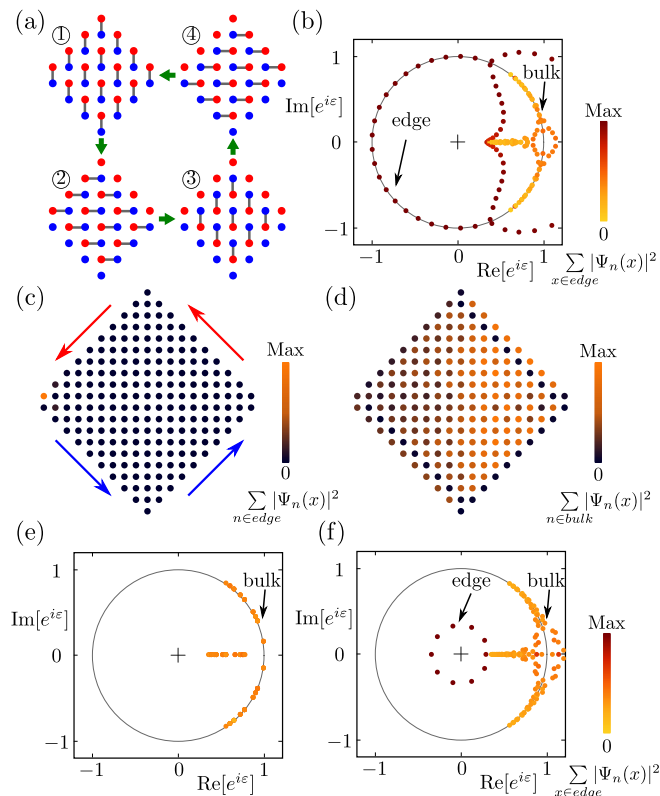


FIG. 6. (Color online) Hybrid skin-topological modes in a non-Hermitian Floquet system with chiral edge states. (a) A periodically driven lattice model proposed in Ref. [89] with gain and loss introduced to two sublattices. (b) Quasi-energies plotted on the complex plane of $e^{i\varepsilon}$ when the system is under OBC. The unit circle is marked where ε is real. Color represents the strength of localization on the left edge $\sum_{x \in \text{edge}} |\Psi_n(x)|^2$. (c) Summation of state densities for all edge states $\sum_{n \in \text{edge}} |\Psi_n(x)|^2$. (d) Summation of state densities for all bulk states $\sum_{n \in \text{bulk}} |\Psi_n(x)|^2$. (e) Same as in panel (b) but under PBC. (f) Same as in panel (b) but the system is under mixed PBC-OBC. The system parameters chosen are $\theta = 0.6\pi$ and $g = 0.5$.

where $U_T(\mathbf{k}) \equiv \mathcal{T} \exp[-i \int_0^T H(\mathbf{k}, \tau) d\tau]$ is the Floquet operator, \mathcal{T} is the time-ordering operator.

Let us first examine the spectrum for both dimensions under OBC. In our calculations, we set $\theta = 0.6\pi$ as an example. For this choice, the system with $g = 0$ supports chiral edge states [81]. With gain and loss at a small strength switched on, the chiral edge states persist. The results for $g = 0.5$ are shown in Fig. 6(b), where a single bulk band and gapless topological edge states are observed. All the edge states are localized at the left corner of the 2D lattice, as shown in Fig. 6(c). By contrast, the bulk states are still extended as shown in Fig. 6(d). All these features are analogous to the previous non-Hermitian Chern insulator case and hence one can expect that hybrid skin-topological modes can be also induced here. In Fig. 6(e) and Fig. 6(f) we also

present the spectrum when the system is under PBC and mixed PBC-OBC, respectively. Again, the energetics of the nonequilibrium chiral edge states are sensitive to the boundary condition, with the PBC-OBC case featuring one clear loop in the spectrum (here we only show the edge states with gain, the edge states with loss out the unit circle also forms a loop).

An auxiliary Hamiltonian approach to nonequilibrium cases

To investigate on a solid ground whether the above-observed corner modes are hybrid skin topological modes, it is necessary to examine the winding behavior of the energetics of the Floquet chiral edge states, again through the emergence of topological corner modes of an auxiliary Hamiltonian. For Floquet systems, it is tempting to define a Floquet Hamiltonian $H_F(\mathbf{k}) = (i/T) \ln(U_T(\mathbf{k}))$, whose eigenvalues are connected with the quasi-energies $\varepsilon(\mathbf{k})$. In this naive approach, an auxiliary Hamiltonian analogous to Eq. (5) can be defined from $H_F(\mathbf{k})$. However, such definition of a Floquet Hamiltonian $H_F(\mathbf{k})$ actually needs to pre-define branch cuts for different quasi-energy gaps in order to take the logarithm operation without ambiguity. In addition, the full topology of a Floquet topological system cannot be captured solely by $H_F(\mathbf{k})$, given that here the Floquet band Chern numbers are zero but there are still chiral edge states [102]. As one contribution of this work, we avoid involving $H_F(\mathbf{k})$ and propose to examine instead the winding behavior of $U_T(\mathbf{k})$.

Specifically, let us now construct the following auxiliary Hamiltonian with the Floquet operator $U_T(\mathbf{k})$ directly,

$$\tilde{H}(\mathbf{k}, \varepsilon_r) = \begin{pmatrix} 0 & U_T(\mathbf{k}) - e^{-i\varepsilon_r} \\ U_T^\dagger(\mathbf{k}) - e^{i\varepsilon_r} & 0 \end{pmatrix}, \quad (13)$$

where ε_r is a real number ranging from 0 to 2π as a reference quasi-energy. By construction, this auxiliary Hamiltonian is Hermitian. Analogous to our previous construction, this auxiliary system also possess the chiral symmetry. The existence of topological corner modes indicates the nontrivial winding of the edge Hamiltonian as k_{\parallel} , the Bloch momentum parallel to the edge, varies over one period. This then suggest the nontrivial winding of the quasi-energy of $U_T(\mathbf{k})$ if one dimension is under OBC and hence the skin effect on the chiral edge states. Note also that our concern here is not about predicting whether there are chiral edge states through a full topological characterization and only spectral winding is important, so the use of $U_T^\dagger(\mathbf{k})$ above suffices to understand the consequences of gain and loss on any existing chiral edge states.

Fig. 7(a) presents the energy bands of $\tilde{H}(\mathbf{k}, \varepsilon_r)$ under a strip structure (mixed PBC-OBC). The edge states

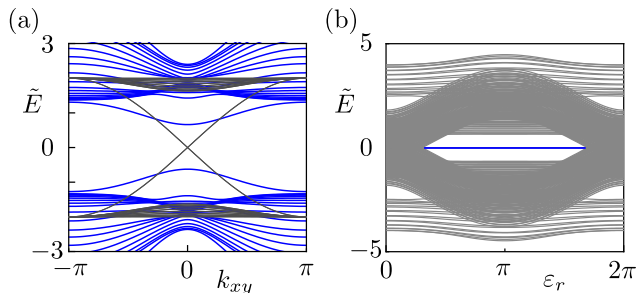


FIG. 7. (Color online) Second-order topological insulator of the auxiliary Hamiltonian associated with the non-Hermitian Floquet model. (a) Energy bands of strip structure for $\varepsilon_r = \pi$. Gray (blue) lines show the results without (with) gain and loss, $g = 0$ ($g = 0.5$). (b) Spectrum of finite structure as a function of reference quasi-energy ε_r . The parameters we used are $\theta = 0.6\pi$ and $g = 0.5$.

are gapless without gain and loss ($g = 0$), as shown by the grey lines. However, upon introducing gain and loss, the edge states of the auxiliary Hamiltonian opens a band gap, as shown by the blue lines. This feature is similar to the previous case constructed from the non-Hermitian Chern insulator, where the gain and loss have induced a topological transition from first-order insulator to second-order insulator. Indeed, if both dimensions are under OBC, this auxiliary system supports topological corner states, as shown in Fig. 7(b). In particular, if the quasi-energy parameter ε_r is in the range of $[0.3\pi, 1.7\pi]$, second-order zero-energy corner states are obtained. This range agrees precisely with that of the quasi-energy of skin corner states plotted on the unit circle in Fig. 6(b). We have thus computationally and conceptually demonstrated that even in nonequilibrium topological systems, the occurrence of hybrid skin-topological modes, which correspond to the winding behavior of the quasi-energy of the edge states when one dimension is under OBC, comes in parallel with second-order topological insulator phase of an auxiliary Hamiltonian constructed directly from the Floquet operator. Our approach here is expected to be widely useful when inspecting the existence of nonequilibrium hybrid skin-topological modes.

DISCUSSION

It is made clear above that the hybrid skin-topological modes arise from the skin effect localization of topological chiral edge states, in both the static and the periodically driven models as case studies. We highlight the similarity and difference between our results and the previous results of hybrid skin-topological modes [17, 46, 58, 59]. In both cases, the number of corner skin modes is proportional to the length of the system and the corner localization appears only if the system is under OBC for two dimensions. However, in previous examples of

skin-topological modes, the role played by two dimensions is entirely separate, one for topological localization and one for skin localization. By contrast, in our generic route here, the two system dimensions are under the same footing, and the obtained skin-topological corner modes are deeply connected with some second-order topological phase induced by gain and loss. Our system is simultaneously a non-Hermitian Chern insulator/non-Hermitian anomalous Floquet topological insulator and supports gapless topological edge state. Furthermore, our proposal is so general that it is extendable to nonequilibrium situations, leading us to the finding of nonequilibrium skin-topological modes.

The two working models considered in this work are highly feasible for experimental studies. Indeed, their Hermitian counterparts (without gain or loss) have already been realized in photonics and acoustics [84, 103–109]. Although in our theoretical considerations we introduce both gain and loss to the system, in real experiments only loss suffices because only the difference between two sublattice sites matters. The loss can be realized by sound/optical absorbing materials or leaky modes [68, 110–114]. In future, it is also interesting to study the discovered mechanism in continuous systems, like topological photonic/phononic crystal [115, 116], instead of lattice models. Considering the seminal Kane-Mele model can be treated as two copies of the Haldane model, it is also possible to find gain and loss induced second-order NHSE in the Kane-Mele model or other valley topological insulators and topological crystal insulators [117].

Acknowledgements: J.G. acknowledges fund support by the Singapore Ministry of Education Academic Research Fund Tier-3 Grant No. MOE2017-T3-1-001 (WBS. No. R-144-000-425-592) and by the Singapore National Research Foundation Grant No. NRF-NRFI2017-04 (WBS No. R-144-000-378-281). We thank Ching Hua Lee and Linhu Li for very helpful discussions.

Appendix A: Symmetry analysis of an auxiliary Hamiltonian associated with the non-Hermitian Haldane model.

In this section, we present our finding that the auxiliary Hamiltonian of our non-Hermitian Haldane model, as defined in the main text, is in fact a fragile topological insulator with fractional charge at its corners. Together with the chiral symmetry of the auxiliary Hamiltonian by construction, this system supports topological corner modes.

In Fig. 8(a), we show the unit cell of the honeycomb lattice and its inversion symmetry points $1a$, $1b$, $1c$ and $1d$. The first Brillouin zone and the inversion symmetric

momentum points Γ, M_1, M_2, M_3 are shown in Fig. 8(b). The elementary band representations of the system can be obtained by putting s or p orbital to the inversion symmetry points and are described by the symmetry eigenvalues at high symmetry momentum points [118]. The elementary band representations are summarized in Table I.

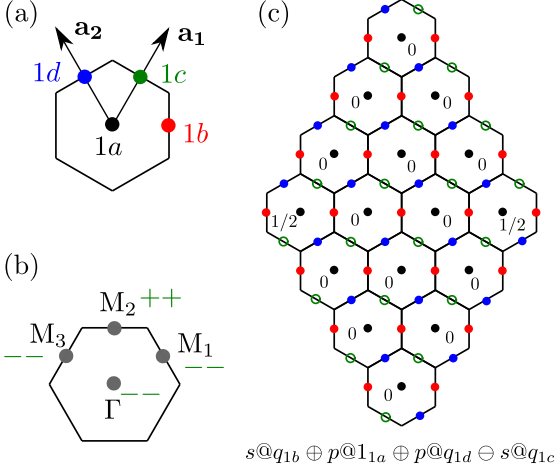


FIG. 8. Fractional charge for the auxiliary Hamiltonian of our non-Hermitian Haldane model. (a) The unit cell of the honeycomb lattice. The inversion symmetry points are marked as $1a, 1b, 1c$ and $1d$. (b) The first Brillouin zone. The inversion symmetry momentum points are marked Γ, M_1, M_2 and M_3 . The symmetry eigenvalues for the auxiliary Hamiltonian of non-Hermitian Haldane model are marked. (c) Two electrons with representation $s@q_{1b} \oplus p@1_{1a} \oplus p@q_{1d} \ominus s@q_{1c}$. The electron charges at different unit cells are indicated mod 1 (in units of the electron charge e).

It is seen that there are two bands below the band gap of the auxiliary Hamiltonian. The symmetry eigenvalues at high symmetry momentum points for $t_1 = 3, t_2 = 0.5, g = 0.6$ and $\phi = \pi/3$ are shown in Fig. 8(b). Compared with the elementary band representations, it is seen that there is no Wannier representation for this auxiliary Hamiltonian. However, we can add one atom orbital $s@q_{1c}$ to the two bands, then it can be represented as three atomic orbital $s@q_{1b} \oplus p@1_{1a} \oplus p@q_{1d}$. This can then be identified as a fragile topological insulator phase, which does not have its Wannier representation but can be Wannierized by adding one atomic orbital. The two bands then can be represented as $s@q_{1b} \oplus p@1_{1a} \oplus p@q_{1d} \ominus s@q_{1c}$.

In Fig. 8(c), we show the charge distribution for the two bands if the system is placed under OBC. The solid circles with color black, blue and red means one orbital at $1a, 1d$ and $1b$, respectively. The open circle with color green means removing one orbital at $1c$. By numbering these sites that keep the inversion symmetry, we can see the fractional charge for the left corner and right corner

TABLE I. Inversion symmetry eigenvalues at high symmetry momentum points for eight elementary band representations of honeycomb lattice with inversion symmetry. Each band representation has either 0, 2 or 4 negative eigenvalues.

	Γ	M_1	M_2	M_3
$s@q_{1a}$	+1	+1	+1	+1
$p@q_{1a}$	-1	-1	-1	-1
$s@q_{1b}$	+1	-1	+1	-1
$p@q_{1b}$	-1	+1	-1	+1
$s@q_{1c}$	+1	-1	-1	+1
$p@q_{1c}$	-1	+1	+1	-1
$s@q_{1d}$	+1	+1	-1	-1
$p@q_{1d}$	-1	-1	+1	+1

is $1/2$. Together with the chiral symmetry, the system supports topological corner modes [88].

Appendix B: Spectrum of the auxiliary Hamiltonian for a non-Hermitian Haldane model with on-site potential difference.

In Fig. 4 of the main text, we already presented the main spectral results for the non-Hermitian Haldane model with on-site potential difference $\mu \sum_{i \in A} c_i^\dagger c_i - \mu \sum_{i \in B} c_i^\dagger c_i$. Here we present more results complementary to Fig. 4. The energy bands of the auxiliary Hamiltonian in zigzag strip structure with $E_r = -t_2$ are shown in Fig. 9(a). When there is no gain/loss, the system supports gapless edge state (grey lines). And the introduction of gain/loss open a band gap to the edge state (blue lines). Due to on-site potential breaking the inversion symmetry, here the spectrum is not symmetric anymore. The spectrum of the auxiliary Hamiltonian under OBC as a function of the reference energy E_r is shown in Fig. 9(b). The system is seen to support zero corner mode for the range $-3.2 \lesssim E_r \lesssim 2.2$, which is fully consistent with the band gap of Fig. 4(a) shown in the main text.

- [1] Ramy El-Ganainy, Konstantinos G. Makris, Mercedeh Khajavikhan, Ziad H. Musslimani, Stefan Rotter, and Demetrios N. Christodoulides, “Non-Hermitian physics and PT symmetry,” *Nature Physics* 2017 14:1 **14**, 11–19 (2018).
- [2] Yuto Ashida, Zongping Gong, and Masahito Ueda, “Non-Hermitian physics,” *Advances in Physics* **69**, 249–435 (2021), arXiv:2006.01837.
- [3] Emil J. Bergholtz, Jan Carl Budich, and Flore K. Kunst, “Exceptional topology of non-Hermitian systems,” *Reviews of Modern Physics* **93**, 015005 (2021), arXiv:1912.10048.

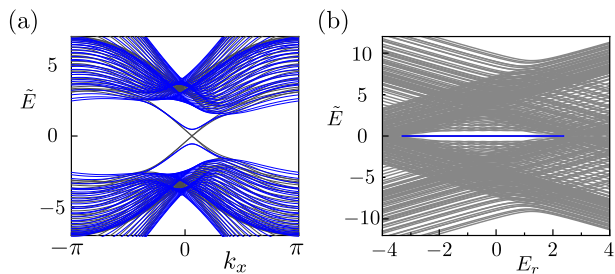


FIG. 9. Second-order topological insulator of the auxiliary Hamiltonian for the non-Hermitian Haldane model with on-site potential difference $\mu \sum_{i \in A} c_i^\dagger c_i - \mu \sum_{i \in B} c_i^\dagger c_i$. (a) Energy bands of zigzag strip structure. Gray (blue) lines show the results without (with) gain and loss, $g = 0$ ($g = 0.6$). The reference energy is $E_r = -t_2$. (b) Spectrum of a finite structure as a function of the reference energy E_r . We choose $t_1 = 3$, $t_2 = 0.5$, $g = 0.6$, $\phi = \pi/3$ and $\mu = 0.5$.

- [4] Zongping Gong, Yuto Ashida, Kohei Kawabata, Kazuaki Takasan, Sho Higashikawa, and Masahito Ueda, “Topological Phases of Non-Hermitian Systems,” *Physical Review X* **8**, 031079 (2018), arXiv:1802.07964.
- [5] Kohei Kawabata, Ken Shiozaki, Masahito Ueda, and Masatoshi Sato, “Symmetry and Topology in Non-Hermitian Physics,” *Physical Review X* **9**, 041015 (2019), arXiv:1812.09133.
- [6] Nobuyuki Okuma, Kohei Kawabata, Ken Shiozaki, and Masatoshi Sato, “Topological Origin of Non-Hermitian Skin Effects,” *Physical Review Letters* **124**, 086801 (2020), arXiv:1910.02878.
- [7] Kai Zhang, Zhesen Yang, and Chen Fang, “Correspondence between winding numbers and skin modes in non-Hermitian systems,” *Physical Review Letters* **125**, 126402 (2020), arXiv:1910.01131.
- [8] Shunyu Yao and Zhong Wang, “Edge States and Topological Invariants of Non-Hermitian Systems,” *Physical Review Letters* **121**, 086803 (2018), arXiv:1803.01876.
- [9] Flore K. Kunst, Elisabet Edvardsson, Jan Carl Budich, and Emil J. Bergholtz, “Biorthogonal Bulk-Boundary Correspondence in Non-Hermitian Systems,” *Physical Review Letters* **121**, 026808 (2018), arXiv:1805.06492.
- [10] A. McDonald, T. Pereg-Barnea, and A. A. Clerk, “Phase-Dependent Chiral Transport and Effective Non-Hermitian Dynamics in a Bosonic Kitaev-Majorana Chain,” *Physical Review X* **8**, 041031 (2018), arXiv:1805.12557.
- [11] Flore K. Kunst and Vatsal Dwivedi, “Non-Hermitian systems and topology: A transfer-matrix perspective,” *Physical Review B* **99**, 245116 (2019), arXiv:1812.02186.
- [12] Stefano Longhi, “Probing non-Hermitian skin effect and non-Bloch phase transitions,” *Physical Review Research* **1**, 023013 (2019), arXiv:1908.07712.
- [13] L. Jin and Z. Song, “Bulk-boundary correspondence in a non-Hermitian system in one dimension with chiral inversion symmetry,” *Physical Review B* **99**, 081103 (2019), arXiv:1809.03139.
- [14] Fei Song, Shunyu Yao, and Zhong Wang, “Non-Hermitian Skin Effect and Chiral Damping in Open Quantum Systems,” *Physical Review Letters* **123**, 170401 (2019), arXiv:1904.08432.
- [15] Ching Hua Lee and Ronny Thomale, “Anatomy of skin modes and topology in non-Hermitian systems,” *Physical Review B* **99**, 201103 (2019), arXiv:1809.02125.
- [16] Dan S. Borgnia, Alex Jura Kruchkov, and Robert Jan Slager, “Non-Hermitian Boundary Modes and Topology,” *Physical Review Letters* **124**, 056802 (2020).
- [17] Ching Hua Lee, Linhu Li, and Jiangbin Gong, “Hybrid Higher-Order Skin-Topological Modes in Nonreciprocal Systems,” *Physical Review Letters* **123**, 016805 (2019), arXiv:1810.11824.
- [18] Tian Shu Deng and Wei Yi, “Non-Bloch topological invariants in a non-Hermitian domain wall system,” *Physical Review B* **100**, 035102 (2019), arXiv:1903.03811.
- [19] Hui Jiang, Li Jun Lang, Chao Yang, Shi Liang Zhu, and Shu Chen, “Interplay of non-Hermitian skin effects and Anderson localization in nonreciprocal quasiperiodic lattices,” *Physical Review B* **100**, 054301 (2019), arXiv:1901.09399.
- [20] Linhu Li, Ching Hua Lee, Sen Mu, and Jiangbin Gong, “Critical non-Hermitian skin effect,” *Nature Communications* **2020** 11:1 **11**, 1–8 (2020), arXiv:2003.03039.
- [21] Ananya Ghatak and Tanmoy Das, “New topological invariants in non-Hermitian systems,” *Journal of Physics: Condensed Matter* **31**, 263001 (2019), arXiv:1902.07972.
- [22] Luis E F Foa Torres, “Perspective on topological states of non-Hermitian lattices,” *Journal of Physics: Materials* **3**, 014002 (2019), arXiv:1909.00809.
- [23] Shunyu Yao, Fei Song, and Zhong Wang, “Non-Hermitian Chern Bands,” *Physical Review Letters* **121**, 136802 (2018), arXiv:1804.04672.
- [24] Kazuki Yokomizo and Shuichi Murakami, “Non-Bloch Band Theory of Non-Hermitian Systems,” *Physical Review Letters* **123**, 066404 (2019), arXiv:1902.10958.
- [25] Ken Ichiro Imura and Yositake Takane, “Generalized bulk-edge correspondence for non-Hermitian topological systems,” *Physical Review B* **100**, 165430 (2019), arXiv:1908.09438.
- [26] Kohei Kawabata, Nobuyuki Okuma, and Masatoshi Sato, “Non-Bloch band theory of non-Hermitian Hamiltonians in the symplectic class,” *Physical Review B* **101**, 195147 (2020), arXiv:2003.07597.
- [27] S. Longhi, “Non-Bloch-Band Collapse and Chiral Zener Tunneling,” *Physical Review Letters* **124**, 066602 (2020), arXiv:2001.10257.
- [28] Colin Scheibner, William T.M. Irvine, and Vincenzo Vitelli, “Non-Hermitian Band Topology and Skin Modes in Active Elastic Media,” *Physical Review Letters* **125**, 118001 (2020), arXiv:2001.04969.
- [29] Xizheng Zhang and Jiangbin Gong, “Non-Hermitian Floquet topological phases: Exceptional points, coalescent edge modes, and the skin effect,” *Physical Review B* **101**, 045415 (2020), arXiv:1909.10234.
- [30] Zhesen Yang, Kai Zhang, Chen Fang, and Jiangping Hu, “Non-Hermitian Bulk-Boundary Correspondence and Auxiliary Generalized Brillouin Zone Theory,” *Physical Review Letters* **125**, 226402 (2020), arXiv:1912.05499.
- [31] Xueyi Zhu, Huaiqiang Wang, Samit Kumar Gupta, Haijun Zhang, Biye Xie, Minghui Lu, and Yanfeng Chen, “Photonic non-Hermitian skin effect and non-Bloch bulk-boundary correspondence,” *Physical Review Research* **2**, 013280 (2020).
- [32] Ananya Ghatak, Martin Brandenbourger, Jasper Van

- Wezel, and Corentin Coulais, “Observation of non-Hermitian topology and its bulk-edge correspondence in an active mechanical metamaterial,” *Proceedings of the National Academy of Sciences of the United States of America* **117**, 29561–29568 (2020), arXiv:1907.11619.
- [33] T. Helbig, T. Hofmann, S. Imhof, M. Abdelghany, T. Kiessling, L. W. Molenkamp, C. H. Lee, A. Szameit, M. Greiter, and R. Thomale, “Generalized bulk–boundary correspondence in non-Hermitian topoelectrical circuits,” *Nature Physics* **2020** 16:7 **16**, 747–750 (2020).
- [34] Lei Xiao, Tianshu Deng, Kunkun Wang, Gaoyan Zhu, Zhong Wang, Wei Yi, and Peng Xue, “Non-Hermitian bulk–boundary correspondence in quantum dynamics,” *Nature Physics* **2020** 16:7 **16**, 761–766 (2020).
- [35] Weiwei Zhu, Wei Xin Teo, Linhu Li, and Jiangbin Gong, “Delocalization of topological edge states,” *Physical Review B* **103**, 195414 (2021), arXiv:2103.04619.
- [36] Longwen Zhou, Yongjian Gu, and Jiangbin Gong, “Dual topological characterization of non-Hermitian Floquet phases,” *Physical Review B* **103**, L041404 (2021), arXiv:2009.13078.
- [37] Deguang Wu, Jiao Xie, Yao Zhou, and Jin An, “Connections between the Open-boundary Spectrum and Generalized Brillouin Zone in Non-Hermitian Systems,” *Physical Review B* **105**, 045422 (2021), arXiv:2110.09259.
- [38] Martin Brandenbourger, Xander Locsin, Edan Lerner, and Corentin Coulais, “Non-reciprocal robotic metamaterials,” *Nature Communications* **2019** 10:1 **10**, 1–8 (2019).
- [39] Tobias Hofmann, Tobias Helbig, Frank Schindler, Nora Salgo, Marta Brzezińska, Martin Greiter, Tobias Kiessling, David Wolf, Achim Vollhardt, Anton Kabaši, Ching Hua Lee, Ante Bilušić, Ronny Thomale, and Titus Neupert, “Reciprocal skin effect and its realization in a topoelectrical circuit,” *Physical Review Research* **2**, 023265 (2020), arXiv:1908.02759.
- [40] Sebastian Weidemann, Mark Kremer, Tobias Helbig, Tobias Hofmann, Alexander Stegmaier, Martin Greiter, Ronny Thomale, and Alexander Szameit, “Topological funneling of light,” *Science* **368**, 311–314 (2020).
- [41] Shuo Liu, Ruiwen Shao, Shaojie Ma, Lei Zhang, Oubo You, Haotian Wu, Yuan Jiang Xiang, Tie Jun Cui, and Shuang Zhang, “Non-Hermitian Skin Effect in a Non-Hermitian Electrical Circuit,” *Research* **2021**, 1–9 (2021).
- [42] Xiujuan Zhang, Yuan Tian, Jian Hua Jiang, Ming Hui Lu, and Yan Feng Chen, “Observation of higher-order non-Hermitian skin effect,” *Nature Communications* **2021** 12:1 **12**, 1–8 (2021).
- [43] Yangyang Chen, Xiaopeng Li, Colin Scheibner, Vincenzo Vitelli, and Guoliang Huang, “Realization of active metamaterials with odd micropolar elasticity,” *Nature Communications* **2021** 12:1 **12**, 1–12 (2021), arXiv:2009.07329.
- [44] Lucas S. Palacios, Serguei Tchoumakov, Maria Guix, Ignacio Pagonabarraga, Samuel Sánchez, and Adolfo G. Grushin, “Guided accumulation of active particles by topological design of a second-order skin effect,” *Nature Communications* **2021** 12:1 **12**, 1–8 (2021), arXiv:2012.14496.
- [45] Li Zhang, Yihao Yang, Yong Ge, Yi Jun Guan, Qiaolu Chen, Qinghui Yan, Fujia Chen, Rui Xi, Yuanzhen Li, Ding Jia, Shou Qi Yuan, Hong Xiang Sun, Hongsheng Chen, and Baile Zhang, “Acoustic non-Hermitian skin effect from twisted winding topology,” *Nature Communications* **2021** 12:1 **12**, 1–7 (2021).
- [46] Deyuan Zou, Tian Chen, Wenjing He, Jiacheng Bao, Ching Hua Lee, Houjun Sun, and Xiangdong Zhang, “Observation of hybrid higher-order skin-topological effect in non-Hermitian topoelectrical circuits,” *Nature Communications* **2021** 12:1 **12**, 1–11 (2021).
- [47] Wengang Zhang, Xiaolong Ouyang, Xianzhi Huang, Xin Wang, Huili Zhang, Yefei Yu, Xiuying Chang, Yanqing Liu, Dong Ling Deng, and L. M. Duan, “Observation of Non-Hermitian Topology with Nonunitary Dynamics of Solid-State Spins,” *Physical Review Letters* **127**, 090501 (2021), arXiv:2012.09191.
- [48] Qian Liang, Dizhou Xie, Zhaoli Dong, Haowei Li, Hang Li, Bryce Gadway, Wei Yi, and Bo Yan, “Observation of Non-Hermitian Skin Effect and Topology in Ultracold Atoms,” (2022), arXiv:2201.09478.
- [49] Kohei Kawabata, Ken Shiozaki, and Masahito Ueda, “Anomalous helical edge states in a non-Hermitian Chern insulator,” *Physical Review B* **98**, 165148 (2018), arXiv:1805.09632.
- [50] Yu Chen and Hui Zhai, “Hall conductance of a non-Hermitian Chern insulator,” *Physical Review B* **98**, 245130 (2018), arXiv:1806.06566.
- [51] Mark R. Hirsbrunner, Timothy M. Philip, and Matthew J. Gilbert, “Topology and observables of the non-Hermitian Chern insulator,” *Physical Review B* **100**, 081104 (2019), arXiv:1901.09961.
- [52] H. C. Wu, L. Jin, and Z. Song, “Inversion symmetric non-Hermitian Chern insulator,” *Physical Review B* **100**, 155117 (2019), arXiv:1905.11576.
- [53] Yi-Xin Xiao and C. T. Chan, “Topology in non-Hermitian Chern insulators with skin effect,” *Physical Review B* **105**, 075128 (2022).
- [54] Xiao Qi Sun, Penghao Zhu, and Taylor L. Hughes, “Geometric Response and Disclination-Induced Skin Effects in Non-Hermitian Systems,” *Physical Review Letters* **127**, 066401 (2021), arXiv:2102.05667.
- [55] Frank Schindler and Abhinav Prem, “Dislocation non-Hermitian skin effect,” *Physical Review B* **104**, L161106 (2021).
- [56] Balaganchi A. Bhargava, Ion Cosma Fulga, Jeroen Van Den Brink, and Ali G. Moghaddam, “Non-Hermitian skin effect of dislocations and its topological origin,” *Physical Review B* **104**, L241402 (2021), arXiv:2106.04567.
- [57] Sourav Manna and Bitan Roy, “Inner Skin Effects on Non-Hermitian Topological Fractals,” (2022), arXiv:2202.07658.
- [58] Linhu Li, Ching Hua Lee, and Jiangbin Gong, “Topological Switch for Non-Hermitian Skin Effect in Cold-Atom Systems with Loss,” *Physical Review Letters* **124**, 250402 (2020).
- [59] Ce Shang, Shuo Liu, Ruiwen Shao, Peng Han, Xiaoning Zang, Xiangliang Zhang, Khaled Nabil Salama, Wenlong Gao, Ching Hua Lee, Ronny Thomale, Aurelien Manchon, Shuang Zhang, Tie Jun Cui, and Udo Schwingenschlogl, “Experimental identification of the second-order non-Hermitian skin effect with physics-graph-informed machine learning,” (2022), 10.48550/arxiv.2203.00484, arXiv:2203.00484.
- [60] Kohei Kawabata, Masatoshi Sato, and Ken Shiozaki,

- “Higher-order non-Hermitian skin effect,” *Physical Review B* **102**, 205118 (2020), arXiv:2008.07237.
- [61] Ryo Okugawa, Ryo Takahashi, and Kazuki Yokomizo, “Second-order topological non-Hermitian skin effects,” *Physical Review B* **102**, 241202 (2020), arXiv:2008.03721.
- [62] Yongxu Fu, Jihan Hu, and Shaolong Wan, “Non-Hermitian second-order skin and topological modes,” *Physical Review B* **103**, 045420 (2021), arXiv:2008.09033.
- [63] Kyoung Min Kim and Moon Jip Park, “Disorder-driven phase transition in the second-order non-Hermitian skin effect,” *Physical Review B* **104**, L121101 (2021), arXiv:2106.13209.
- [64] Kenta Takata and Masaya Notomi, “Photonic Topological Insulating Phase Induced Solely by Gain and Loss,” *Physical Review Letters* **121**, 213902 (2018).
- [65] Xi-Wang Luo and Chuanwei Zhang, “Higher-Order Topological Corner States Induced by Gain and Loss,” *Physical Review Letters* **123**, 073601 (2019).
- [66] Yutian Ao, Xiaoyong Hu, Yilong You, Cuicui Lu, Yulan Fu, Xingyuan Wang, and Qihuang Gong, “Topological Phase Transition in the Non-Hermitian Coupled Resonator Array,” *Physical Review Letters* **125** (2020), 10.1103/PHYSREVLETT.125.013902.
- [67] Alex Y. Song, Xiao Qi Sun, Avik Dutt, Momchil Minkov, Casey Wojcik, Haiwen Wang, Ian A.D. Williamson, Meir Orenstein, and Shanhui Fan, “P T-Symmetric Topological Edge-Gain Effect,” *Physical Review Letters* **125** (2020), 10.1103/PHYSREVLETT.125.033603/FIGURES/2/THUMBNAI.
- [68] He Gao, Haoran Xue, Zhongming Gu, Tuo Liu, Jie Zhu, and Baile Zhang, “Non-Hermitian route to higher-order topology in an acoustic crystal,” *Nature Communications* 2021 12:1 **12**, 1–7 (2021), arXiv:2007.01041.
- [69] Sebastian Weidemann, Mark Kremer, Stefano Longhi, and Alexander Szameit, “Topological triple phase transition in non-Hermitian Floquet quasicrystals,” *Nature* 2022 601:7893 **601**, 354–359 (2022).
- [70] Wladimir A. Benalcazar, B. Andrei Bernevig, and Taylor L. Hughes, “Quantized electric multipole insulators,” *Science* **357**, 61–66 (2017), arXiv:1611.07987.
- [71] Christopher W. Peterson, Wladimir A. Benalcazar, Taylor L. Hughes, and Gaurav Bahl, “A quantized microwave quadrupole insulator with topologically protected corner states,” *Nature* 2018 555:7696 **555**, 346–350 (2018).
- [72] Marc Serra-Garcia, Valerio Peri, Roman Süsstrunk, Osama R. Bilal, Tom Larsen, Luis Guillermo Villanueva, and Sebastian D. Huber, “Observation of a phononic quadrupole topological insulator,” *Nature* 2018 555:7696 **555**, 342–345 (2018), arXiv:1708.05015.
- [73] Stefan Imhof, Christian Berger, Florian Bayer, Johannes Brehm, Laurens W. Molenkamp, Tobias Kiessling, Frank Schindler, Ching Hua Lee, Martin Greiter, Titus Neupert, and Ronny Thomale, “Topoelectrical-circuit realization of topological corner modes,” *Nature Physics* 2018 14:9 **14**, 925–929 (2018), arXiv:1708.03647.
- [74] Sunil Mittal, Venkata Vikram Orre, Guanyu Zhu, Maxim A. Gorlach, Alexander Poddubny, and Mohammad Hafezi, “Photonic quadrupole topological phases,” *Nature Photonics* 2019 13:10 **13**, 692–696 (2019), arXiv:1812.09304.
- [75] Bi Ye Xie, Guang Xu Su, Hong Fei Wang, Hai Su, Xiao Peng Shen, Peng Zhan, Ming Hui Lu, Zhen Lin Wang, and Yan Feng Chen, “Visualization of Higher-Order Topological Insulating Phases in Two-Dimensional Dielectric Photonic Crystals,” *Physical Review Letters* **122**, 233903 (2019), arXiv:1812.06263.
- [76] Xiao Dong Chen, Wei Min Deng, Fu Long Shi, Fu Li Zhao, Min Chen, and Jian Wen Dong, “Direct Observation of Corner States in Second-Order Topological Photonic Crystal Slabs,” *Physical Review Letters* **122**, 233902 (2019), arXiv:1812.08326.
- [77] Feng Liu, Katsunori Wakabayashi, Katsuyuki Watanabe, Ryota Katsumi, Satoshi Iwamoto, Yasuhiko Arakawa, and Yasutomo Ota, “Photonic crystal nanocavity based on a topological corner state,” *Optica*, Vol. 6, Issue 6, pp. 786–789 **6**, 786–789 (2019).
- [78] Haoran Xue, Yahui Yang, Fei Gao, Yidong Chong, and Baile Zhang, “Acoustic higher-order topological insulator on a kagome lattice,” *Nature Materials* 2018 18:2 **18**, 108–112 (2018), arXiv:1806.09418.
- [79] Xiang Ni, Matthew Weiner, Andrea Alù, and Alexander B. Khanikaev, “Observation of higher-order topological acoustic states protected by generalized chiral symmetry,” *Nature Materials* 2018 18:2 **18**, 113–120 (2018).
- [80] Xiujuan Zhang, Hai Xiao Wang, Zhi Kang Lin, Yuan Tian, Biye Xie, Ming Hui Lu, Yan Feng Chen, and Jian Hua Jiang, “Second-order topology and multidimensional topological transitions in sonic crystals,” *Nature Physics* 2019 15:6 **15**, 582–588 (2019).
- [81] Weiwei Zhu, Y. D. Chong, and Jiangbin Gong, “Floquet higher-order topological insulator in a periodically driven bipartite lattice,” *Physical Review B* **103**, L041402 (2021), arXiv:2010.03879.
- [82] Linhu Li, Weiwei Zhu, and Jiangbin Gong, “Direct dynamical characterization of higher-order topological phases with nested band inversion surfaces,” *Science Bulletin* **66**, 1502–1510 (2021), arXiv:2007.05759.
- [83] Jingjing Niu, Tongxing Yan, Yuxuan Zhou, Ziyu Tao, Xiaole Li, Weiyang Liu, Libo Zhang, Hao Jia, Song Liu, Zhongbo Yan, Yuanzhen Chen, and Dapeng Yu, “Simulation of higher-order topological phases and related topological phase transitions in a superconducting qubit,” *Science Bulletin* **66**, 1168–1175 (2021), arXiv:2001.03933.
- [84] Weiwei Zhu, Haoran Xue, Jiangbin Gong, Yidong Chong, and Baile Zhang, “Time-periodic corner states from Floquet higher-order topology,” *Nature Communications* 2022 13:1 **13**, 1–6 (2022), arXiv:2012.08847.
- [85] Max Geier, Luka Trifunovic, Max Hoskam, and Piet W. Brouwer, “Second-order topological insulators and superconductors with an order-two crystalline symmetry,” *Physical Review B* **97**, 205135 (2018), arXiv:1801.10053.
- [86] F. D.M. Haldane, “Model for a Quantum Hall Effect without Landau Levels: Condensed-Matter Realization of the “Parity Anomaly”,” *Physical Review Letters* **61**, 2015 (1988).
- [87] Hoi Chun Po, Haruki Watanabe, and Ashvin Vishwanath, “Fragile Topology and Wannier Obstructions,” *Physical Review Letters* **121**, 126402 (2018), arXiv:1709.06551.
- [88] Wladimir A. Benalcazar, Tianhe Li, and Taylor L. Hughes, “Quantization of fractional corner charge in C_n-symmetric higher-order topological crystalline insulators,” *Physical Review B* **99**, 245151 (2019),

- arXiv:1809.02142.
- [89] Mark S. Rudner, Netanel H. Lindner, Erez Berg, and Michael Levin, “Anomalous edge states and the bulk-edge correspondence for periodically driven two-dimensional systems,” *Physical Review X* **3**, 031005 (2013), arXiv:1212.3324.
- [90] Takuya Kitagawa, Erez Berg, Mark Rudner, and Eugene Demler, “Topological characterization of periodically driven quantum systems,” *Physical Review B - Condensed Matter and Materials Physics* **82**, 235114 (2010), arXiv:1010.6126.
- [91] Derek Y.H. Ho and Jiangbin Gong, “Quantized adiabatic transport in momentum space,” *Physical Review Letters* **109**, 010601 (2012).
- [92] A. Gómez-León and G. Platero, “Floquet-Bloch Theory and Topology in Periodically Driven Lattices,” *Physical Review Letters* **110**, 200403 (2013), arXiv:1303.4369.
- [93] Arijit Kundu and Babak Seradjeh, “Transport signatures of floquet majorana fermions in driven topological superconductors,” *Physical Review Letters* **111**, 136402 (2013), arXiv:1301.4433.
- [94] Mahmoud Lababidi, Indubala I. Satija, and Erhai Zhao, “Counter-propagating edge modes and topological phases of a kicked quantum hall system,” *Physical Review Letters* **112**, 026805 (2014), arXiv:1307.3569.
- [95] L. E.F. Foa Torres, P. M. Perez-Piskunow, C. A. Balsero, and Gonzalo Usaj, “Multiterminal conductance of a floquet topological insulator,” *Physical Review Letters* **113**, 266801 (2014), arXiv:1409.2482.
- [96] Hannes Hübener, Michael A. Sentef, Umberto De Giovannini, Alexander F. Kemper, and Angel Rubio, “Creating stable Floquet-Weyl semimetals by laser-driving of 3D Dirac materials,” *Nature Communications* **2017** 8:1 **8**, 1–8 (2017), arXiv:1604.03399.
- [97] Longwen Zhou and Jiangbin Gong, “Recipe for creating an arbitrary number of Floquet chiral edge states,” *Physical Review B* **97**, 245430 (2018), arXiv:1804.06407.
- [98] J. W. McIver, B. Schulte, F. U. Stein, T. Matsuyama, G. Jotzu, G. Meier, and A. Cavalleri, “Light-induced anomalous Hall effect in graphene,” *Nature Physics* **2019** 16:1 **16**, 38–41 (2019), arXiv:1811.03522.
- [99] Mark S. Rudner and Netanel H. Lindner, “Band structure engineering and non-equilibrium dynamics in Floquet topological insulators,” *Nature Reviews Physics* **2020** 2:5 **2**, 229–244 (2020).
- [100] Karen Wintersperger, Christoph Braun, F. Nur Ünal, André Eckardt, Marco Di Liberto, Nathan Goldman, Immanuel Bloch, and Monika Aidelsburger, “Realization of an anomalous Floquet topological system with ultracold atoms,” *Nature Physics* **2020** 16:10 **16**, 1058–1063 (2020), arXiv:2002.09840.
- [101] Michael Pasek and Y. D. Chong, “Network models of photonic Floquet topological insulators,” *Physical Review B - Condensed Matter and Materials Physics* **89**, 075113 (2014), arXiv:1311.4789.
- [102] Weiwei Zhu, Y. D. Chong, and Jiangbin Gong, “Symmetry analysis of anomalous Floquet topological phases,” *Physical Review B* **104**, L020302 (2021), arXiv:2103.08230.
- [103] Mikael C. Rechtsman, Julia M. Zeuner, Yonatan Plotnik, Yaakov Lumer, Daniel Podolsky, Felix Dreisow, Stefan Nolte, Mordechai Segev, and Alexander Szameit, “Photonic Floquet topological insulators,” *Nature* **2013** 496:7444 **496**, 196–200 (2013), arXiv:1212.3146.
- [104] Fei Gao, Zhen Gao, Xihang Shi, Zhaoju Yang, Xiao Lin, Hongyi Xu, John D. Joannopoulos, Marin Soljačić, Hongsheng Chen, Ling Lu, Yidong Chong, and Baile Zhang, “Probing topological protection using a designer surface plasmon structure,” *Nature Communications* **2016** 7:1 **7**, 1–9 (2016).
- [105] Yu Gui Peng, Cheng Zhi Qin, De Gang Zhao, Ya Xi Shen, Xiang Yuan Xu, Ming Bao, Han Jia, and Xue Feng Zhu, “Experimental demonstration of anomalous Floquet topological insulator for sound,” *Nature Communications* **2016** 7:1 **7**, 1–8 (2016).
- [106] Sebrata Mukherjee, Alexander Spracklen, Manuel Valiente, Erika Andersson, Patrik Öberg, Nathan Goldman, and Robert R. Thomson, “Experimental observation of anomalous topological edge modes in a slowly driven photonic lattice,” *Nature Communications* **2017** 8:1 **8**, 1–7 (2017), arXiv:1604.05612.
- [107] Lukas J. Maczewsky, Julia M. Zeuner, Stefan Nolte, and Alexander Szameit, “Observation of photonic anomalous Floquet topological insulators,” *Nature Communications* **2017** 8:1 **8**, 1–7 (2017), arXiv:1605.03877.
- [108] Sunil Mittal, Venkata Vikram Orre, Daniel Leykam, Y. D. Chong, and Mohammad Hafezi, “Photonic Anomalous Quantum Hall Effect,” *Physical Review Letters* **123**, 043201 (2019), arXiv:1904.01090.
- [109] Shirin Afzal, Tyler J. Zimmerling, Yang Ren, David Perron, and Vien Van, “Realization of Anomalous Floquet Insulators in Strongly Coupled Nanophotonic Lattices,” *Physical Review Letters* **124**, 253601 (2020), arXiv:1912.10126.
- [110] Kun Ding, Guancong Ma, Meng Xiao, Z. Q. Zhang, and C. T. Chan, “Emergence, coalescence, and topological properties of multiple exceptional points and their experimental realization,” *Physical Review X* **6**, 021007 (2016).
- [111] Jiho Noh, Sheng Huang, Daniel Leykam, Y. D. Chong, Kevin P. Chen, and Mikael C. Rechtsman, “Experimental observation of optical Weyl points and Fermi arc-like surface states,” *Nature Physics* **2017** 13:6 **13**, 611–617 (2017).
- [112] L. Xiao, X. Zhan, Z. H. Bian, K. K. Wang, X. Zhang, X. P. Wang, J. Li, K. Mochizuki, D. Kim, N. Kawakami, W. Yi, H. Obuse, B. C. Sanders, and P. Xue, “Observation of topological edge states in parity-time-symmetric quantum walks,” *Nature Physics* **2017** 13:11 **13**, 1117–1123 (2017).
- [113] Weiwei Zhu, Xinsheng Fang, Dongting Li, Yong Sun, Yong Li, Yun Jing, and Hong Chen, “Simultaneous Observation of a Topological Edge State and Exceptional Point in an Open and Non-Hermitian Acoustic System,” *Physical Review Letters* **121**, 124501 (2018), arXiv:1803.04110.
- [114] K. Özdemir, S. Rotter, F. Nori, and L. Yang, “Parity-time symmetry and exceptional points in photonics,” *Nature Materials* **2019** 18:8 **18**, 783–798 (2019).
- [115] Tomoki Ozawa, Hannah M. Price, Alberto Amo, Nathan Goldman, Mohammad Hafezi, Ling Lu, Mikael C. Rechtsman, David Schuster, Jonathan Simon, Oded Zilberberg, and Iacopo Carusotto, “Topological photonics,” *Reviews of Modern Physics* **91**, 015006 (2019), arXiv:1802.04173.

- [116] Guancong Ma, Meng Xiao, and C. T. Chan, “Topological phases in acoustic and mechanical systems,” *Nature Reviews Physics* 2019 1:4 **1**, 281–294 (2019).
- [117] Xiao Liang Qi and Shou Cheng Zhang, “Topological insulators and superconductors,” *Reviews of Modern Physics* **83**, 1057 (2011), arXiv:1008.2026.
- [118] Jennifer Cano and Barry Bradlyn, “Band Representations and Topological Quantum Chemistry,” *Annu. Rev. Condens. Matter Phys.* **12**, 225–246 (2021), arXiv:2006.04890.